



Working Paper Series

Long-term Effects of Redlining on Climate Risk Exposure

WP 22-09R

Claire Conzelmann
University of Chicago

Arianna Salazar-Miranda
MIT

Toàn Phan
Federal Reserve Bank of Richmond

Jeremy Hoffman
Groundwork USA

This paper can be downloaded without charge
from: <http://www.richmondfed.org/publications/>



Richmond • Baltimore • Charlotte

Long-term Effects of Redlining on Climate Risk Exposure

Claire Conzelmann^a, Arianna Salazar-Miranda^b, Toàn Phan^{*c}, and Jeremy Hoffman^d

^aUniversity of Chicago, Chicago, IL

^bMIT, Department of Urban Studies and Planning, Cambridge, MA

^cFederal Reserve Bank of Richmond, Research Department, Richmond, VA

^cGroundwork USA, Yonkers, NY

September 14, 2023

Abstract

Climate change amplifies environmental hazards, including extreme precipitation and heat events. These hazards are further exacerbated by urban design features like impervious land surfaces and insufficient tree cover. While the enduring socioeconomic impacts of redlining—a policy that systematically denied financial services to specific neighborhoods—are well-studied, its long-term effects on vulnerability to climate risks remain under-explored. Using a boundary design methodology, our study examines 202 U.S. cities and reveals that neighborhoods that were redlined in the 1930s-1940s by the Home Owners’ Loan Corporation face disproportionately higher risks of both current and future flooding and extreme heat. These heightened vulnerabilities are at least partly due to diminished environmental capital in the present day—most notably, reduced tree canopy and lower ground surface permeability. Our findings underscore the persistent and far-reaching influence of historical redlining policies in shaping unequal climate risk exposure.

Keywords: climate risk, flood risk, redlining, environmental justice.

*The views expressed here are those of the authors and should not be interpreted as those of the Federal Reserve Bank of Richmond or the Federal Reserve System. We thank Dan Aaronson, Dan Hartley, and Leah Plachinski for sharing historical data with us. Brooke Hansbrough provided excellent research assistance. All errors are ours. We have no funding to declare. Contacts: ariana@mit.edu, cconzelmann@uchicago.edu, toan.phan@rich.frb.org, jeremy@groundworkusa.org.

1 Introduction

The legacy of policies enacted nearly a century ago may still persist in American society, even after their formal discontinuation. A prominent example is the “redlining” policy implemented by the Home Owners’ Loan Corporation (HOLC) in the 1930s.¹ This policy employed maps to assess neighborhood lending risks and was outlawed in the 1960s due to its discriminatory nature. Although designed to assess financial lending risk factors such as housing age and property values, these maps also took into account the racial makeup of neighborhoods and have been linked to declines in homeownership rates, property values, and rents in areas that received lower grades.^{2,3}

While existing literature has actively debated the influence of redlining on contemporary income and wealth disparities,^{2–8} limited research has delved into the policy’s long term impact on vulnerability to environmental and climate risks. Addressing this gap is critical for ongoing efforts¹ aimed at reducing environmental, health, and economic disparities across diverse communities.^{10,11}

Our study contributes new evidence into the effects of redlining on present-day exposure to climate-related risks. By integrating digitized HOLC maps with high-resolution climate risk data, we focus on assessing exposure to both present and future flooding and extreme heat. The study leverages the granular nature of HOLC grading throughout cities, which allows for a quasi-natural experiment: similar properties divided by HOLC boundaries end up being assigned different risk grades, providing a unique avenue for estimating the policy’s enduring impacts.

Utilizing a boundary design that compares properties in contiguous HOLC boundaries with different grades, we establish a direct relationship between lower HOLC grades and increased flood and heat risks. Properties on the lower-graded side of a HOLC boundary exhibit a *flood factor* 0.1 points higher than those on the higher-graded side, equating to a 5.5% increase in flood risk relative to the sample mean. Additionally, we find a similar but smaller difference in heat risk. Specifically, the *heat factor* increases by 0.011 points on the lower-graded side of a HOLC boundary. All of our estimates are precisely estimated with statistical significance at the 1% level.

Further, we examine potential mechanisms driving these differences. We document that lower-graded areas have weaker *environmental capital*, i.e., the stock of environmental quality factors that mediate and determine the exposure to environmental risks in the present day. To proxy for environmental capital, we use tree canopy coverage and ground surface perviousness: two factors that depend on local public and private investments and have been shown to reduce environmental risks.^{12–14} We find that properties on the lower-graded side of a HOLC

¹Including the recent proposal by federal bank regulatory agencies to strengthen and modernize the Community Reinvestment Act to better serve the needs of low- and moderate-income neighborhoods.⁹

boundary have less tree canopy and lower perviousness than properties on the higher-graded side. We interpret these local differences as reflecting a lack of investments in environmental capital on lower-graded sides of HOLC boundaries.

This paper contributes to two primary bodies of research. First, it augments existing literature on the enduring impacts of historical redlining on present-day socioeconomic conditions. Recent papers have shown that HOLC maps may not have directly influenced mortgage allocation^{15,16}, but are linked to adverse housing outcomes, such as reduced homeownership and economic opportunity.^{2,3,7,17,18} Our work diverges by providing causal evidence of redlining’s impact on environmental risks.

Second, we contribute to the literature on environmental justice. This literature has shown that racial and ethnic minorities, as well as lower-income communities, are disproportionately exposed to environmental hazards like heat, air pollution, and flooding.¹⁹⁻²⁴ Closer to our paper is work showing that redlined neighborhoods experience elevated levels of land surface urban heat.^{25,26} Our study advances this line of inquiry by providing rigorous evidence on the causal effects of historical redlining policies on contemporary climate risk exposure. Moreover, we identify a key mechanism underlying this disparity: reduced investments in environmental capital in redlined areas.

2 Method

2.1 Data

Historical HOLC Maps We acquired shapefiles of HOLC maps from the University of Richmond’s Digital Scholarship Lab’s through their [Mapping Inequality database](#). This project has digitized historical HOLC maps encompassing 239 cities. The maps display neighborhood grades, which span from A (indicating the lowest lending risk and highest stability) to D (representing the highest lending risk and lowest stability). Neighborhoods are color-coded—green for A, blue for B, yellow for C, and red for D—giving rise to the term “redlining.” Our analysis focuses on 202 cities across the U.S., where each neighborhood has been assigned a HOLC grade from A to D. Figure [SI1](#) showcases examples of the HOLC maps across multiple cities.

High-Resolution Measures of Contemporary Exposure to Climate Risks We focus on two key climate-related risks: flooding and heat exposure. To quantify flood risk, we leverage a proprietary dataset from the [First Street Foundation](#). This dataset offers state-of-the-art flood risk projections at the property level using their standardized *flood factor*, a composite score reflecting both the severity and cumulative likelihood of flooding over a 30-year period from 2021 to 2050. The *flood factor* is generated by their First Street Foundation

Flood Model^{27,28}. This model takes into account four major flood contributors: rainfall, river overflow, high tide, and coastal storm surge. It also adjusts for local variables such as elevation, ground surface perviousness, and existing community flood protection measures like dunes, wetlands, and seawalls. Importantly, the model is forward-looking, explicitly considering projected climate change effects, including sea-level rise.

For heat exposure, we use First Street Foundation’s *heat factor*, calculated through their Extreme Heat Model²⁹. The model utilizes temperature and humidity data sourced from the US Geological Service (USGS) and the National Oceanic and Atmospheric Association (NOAA) to produce a high-resolution forecast of the average high “feels like” temperature for the hottest month of summer. The model also incorporates future scenarios by exploring multiple outcomes under the RCP 4.5 carbon emissions pathway, thus projecting temperature changes for the next 30 years. For each property, the *heat factor* is determined as the average “feels like” temperature for the month of July over this 30-year forecast period.

Both the *flood factor* and the *heat factor* are risk scores scaled from 1 to 10, with a value of one indicating the lowest risk and a value of ten indicating the highest risk. Figure SI2 provides a visualization of these two factors.

High-Resolution Measures of Contemporary Environmental Capital We examine two critical aspects of environmental capital: tree coverage and ground surface perviousness. To measure tree coverage, we utilize the *tree canopy cover* data from the [National Land Cover Database \(NLCD\)](#), which provides the percentage of tree canopy coverage in each 30m×30m cell using NASA/USGS Landsat imagery from 2016.

To measure ground surface imperviousness, we use the [NLCD 2016 Urban Imperviousness database](#), which calculates the fraction of developed land that employs impervious surfaces in 30m×30m cells. For ease of interpretation, we use a *perviousness* index for each cell, defined as one minus the imperviousness share.

Geographic Factors We also incorporate data for several key geographic attributes. For slope and elevation, we use data from the USGS, which provides raster data on elevation in meters above the sea level available for 1/3 arc-second cells (approximately 10m cells). The inclination of slope is calculated in degrees. The values range from 0 to 90. For precipitation, we use data on annual precipitation from the USDA available for 800m grids and measured in inches of precipitation per year.

Summary Statistics Table 1 presents summary statistics and the sample sizes for our measures of environmental risk and capital for the cities in our sample and by HOLC grade. The bottom panel of the table shows that, on average, as one moves from a higher-graded cell to lower-graded one, there is a sizable decline in our proxies of environmental capital. For

example, tree canopy coverage declines from 25.8% to 8.4%, and perviousness decreases from 65.3% to 42.4% as we move from A-graded to D-graded neighborhoods.

The differences in environmental risk across grades are less discernible since they might also capture differences in geographic attributes that vary across locations, such as elevation or coastal proximity. For example, A-graded properties could have a greater flood risk because they are in high-income neighborhoods near the coast relative to D-graded properties in more inland neighborhoods. To separate the role of redlining from other geographic differences, we implement a boundary design that compares similar properties on opposite sides of HOLC boundaries.

Table 1: SUMMARY STATISTICS

	(I)	(II)	(III)	(IV)	(V)	(VI)
	Full Sample	A grade	B grade	C grade	D grade	100m Boundary Sample
<i>Panel A. Climate Risk Factors</i>						
Flood Factor (1-10)	1.83 (1.98)	1.73 (1.97)	1.66 (1.81)	1.79 (1.91)	2.09 (2.23)	1.83 (2.02)
Observations (properties)	11,386,565	821,879	2,613,183	5,022,244	2,886,924	2,014,576
Heat Factor (1-10)	4.71 (2.04)	4.58 (2.04)	4.65 (1.99)	4.59 (1.99)	5.03 (2.13)	4.64 (2.06)
Observations (properties)	11,402,312	822,597	2,613,862	5,030,555	2,892,959	2,017,105
<i>Panel B. Environmental Capital Factors</i>						
Tree Canopy (%)	13.10 (21.12)	25.79 (26.05)	16.01 (22.32)	11.41 (19.35)	8.42 (18.15)	12.41 (19.95)
Observations (30m cells)	13,843,586	1,420,253	3,014,739	5,761,008	3,647,586	2,360,390
Perviousness (%)	48.05 (27.29)	65.29 (24.63)	52.19 (25.58)	45.18 (26.09)	42.44 (28.29)	45.67 (25.64)
Observations (30m cells)	13,843,586	1,420,253	3,014,739	5,761,008	3,647,586	2,360,390

Note.— The table provides the mean and standard deviation (in parentheses) for the measures of environmental risk and the proxies for environmental capital. The columns break down these statistics by sample, including all HOLC areas in our cities: A-graded areas, B-graded areas, C-graded areas, and D-graded areas, respectively. The final column reports these statistics for the 100m boundary sample described in Section 2.

2.2 Boundary Discontinuity Method

Ideally, we would like to compare the climate risks of otherwise similar neighborhoods that were randomly assigned different HOLC grades. To approximate this, we adopt a boundary discontinuity design that compares pairs of similar observations lying close to the HOLC boundary on opposite sides and hence are assigned different HOLC grades. [2,3,30,31](#)

We construct the boundary sample following these steps. First, we selected HOLC boundaries that demarcate neighborhoods with differing grades. For simplicity, these boundaries were decomposed into straight line segments, referred to as *borders*. Next, we focused on observations—properties or cells—whose centroids were within a 100m radius of these borders. For robustness, we also considered 50m and 200m buffers (refer to Section 3.3 for further details).²

Figure 1 visualizes our sample construction. Panel (a) shows the HOLC map of Baltimore and identifies the borders between polygons of differing grades and their corresponding 100m buffers. Panel (b) shows an enlarged map of a selection of the HOLC polygons in Baltimore. The thicker lines represent the HOLC border separating differently graded polygons. The thinner lines show the 100m buffer zones around each border. The black and grey points denote the set of properties within the 100m buffers. The black points are properties on the higher-graded side of the nearest HOLC border; the grey points are properties on the lower-graded side of the nearest HOLC border.

One potential concern with our boundary design is that the neighborhoods might not be representative of all areas that received a HOLC grade. The last column in Table 1 provides the summary statistics for the 100m boundary sample. It shows that the mean and standard deviation of the measures of climate risks and environmental capital in this subsample are comparable to those of the full sample, as reported in column 1. This alleviates the concern that the boundary sample is not representative of the full sample.

Using the 100m boundary sample, we then estimate the effect of a lower HOLC grade by comparing properties on opposite sides of the same border (i.e., the properties lying on opposite sides of the border identified with black or grey dots in Figure 1). Key to identification is the *continuity assumption*, which supposes that the relationship between the dependent variable (environmental risks in our case) and the independent variable (HOLC grades) remains continuous (i.e., does not have any abrupt change or discontinuity) at the boundary. In our context, this assumption presupposes that observations on different sides of a border have similar *location fundamentals*—geographic attributes that determine the location’s exposure to environmental risks in the long run. Whether a property happens to lie on a higher or lower-graded side is thus an exogenous source of variation in the assignment of HOLC grades.

To check the continuity assumption, we examine how properties differ in their key geographic attributes: elevation, precipitation, and slope. Table 2 reports summary statistics of these location fundamentals for our boundary sample. Columns 1 and 2 report these statistics for higher- and lower-graded sides of the HOLC borders, respectively. The third column re-

²Distances were computed differently based on the variable type. For property-level flood factor and heat factor variables, we compute the distance from each property’s centroid to the nearest HOLC border. For cell-level variables, such as tree canopy and ground surface perviousness, we computed the distance from each cell’s centroid to the nearest HOLC border.

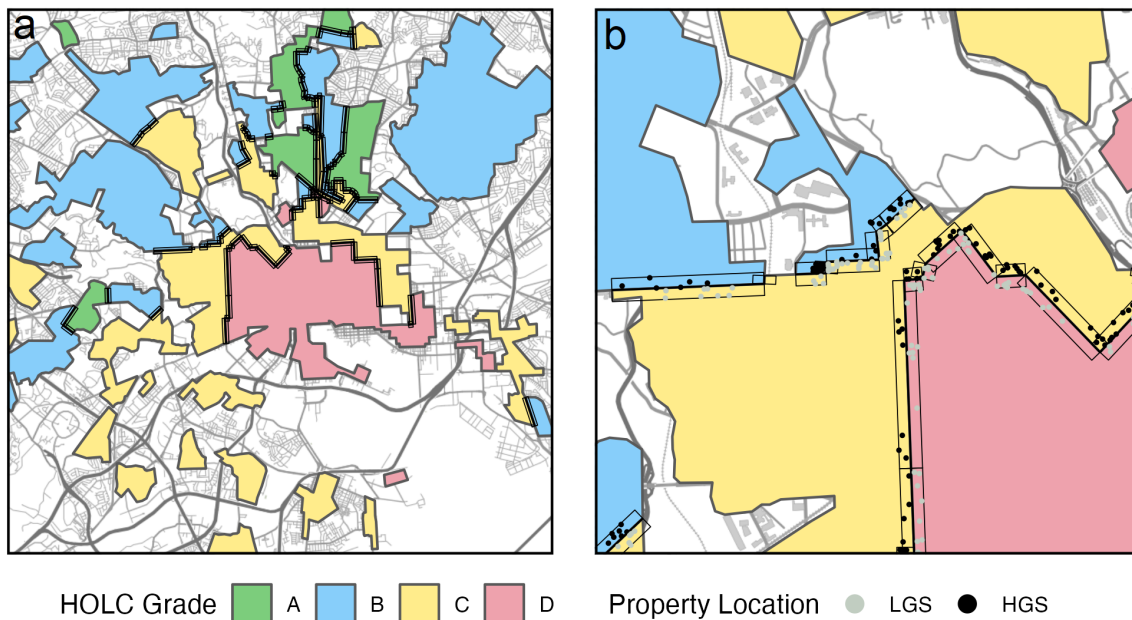


Figure 1: A VISUALIZATION OF SAMPLE CONSTRUCTION. Panel (a) shows the HOLC map of Baltimore with borders and buffer zones between polygons with differing HOLC grades. Panel (b) shows an enlarged map of a sample of the HOLC borders in Baltimore. The thicker lines represent the HOLC border separating differently graded polygons. The thinner lines are 100m buffer zones around each border. Only observations (properties or cells) with centroids within the 100m buffer zones are included in the sample. The map also shows as dots a random subsample of properties for illustration; the black dots are on the higher-graded side of the HOLC border, while the grey dots are on the lower-graded side of the HOLC border.

ports the difference between these means and its standard error. This standard error is robust to two-way clustering at the county and border levels to account for spatial correlation. Differences in all fundamentals are small, and with the exception of elevation, not statistically significant. However, even in this case, differences in elevation between higher and lower-graded sides are only 2.8 meters above sea level—less than 2% of the sample average. The evidence in this Table shows that there are no relevant differences in location fundamentals across opposite sides of the HOLC borders.

To study the long-term effects of redlining on contemporary exposure to climate risks, we estimate the following regression using the boundary sample:

$$\text{Climate Risk}_i = \alpha + \beta_B B_i + \beta_C C_i + \beta_D D_i + f_b + \epsilon_i. \quad (1)$$

Table 2: SUMMARY STATISTICS OF LOCATION FUNDAMENTALS IN BOUNDARY SAMPLE

	100M BOUNDARY SAMPLE		
	Higher-Graded Side	Lower-Graded Side	Difference (Higher vs Lower)
Elevation	181.01	178.21	2.80 (1.44)
Observations	1,003,848	1,013,429	
Precipitation	38.90	39.09	-0.183 (0.141)
Observations (800m cells)	1,003,860	1,013,454	
Slope	0.60	0.59	0.0036 (0.005)
Observations (10m cells)	1,003,860	1,013,454	

Note.— The table provides the average of each variable on the higher- and lower-graded sides of HOLC borders and the difference in means. Standard errors allowing for two-way clustering at the county and border levels are in parentheses. The boundary sample includes observations within 100m of a HOLC border in areas with different HOLC grades. Elevation is in meters above sea level. Precipitation measures annual rainfall per year in inches. Slope represents the rate of change of elevation and is calculated in degrees.

We use flooding and heat factors as our measures of climate risk. For each outcome, i denotes a property, and we estimate equation (1) at the property level.

The regression explains climate risk as a function of HOLC grades, treating a grade of A as the excluded category. The dummy variables B_i, C_i , and D_i indicate the HOLC grade of the area that contains each observation i . The coefficients β_B, β_C , and β_D capture the causal effect of being assigned a grade lower than A. We control for border fixed effects f_b , where b is the closest HOLC border to property i . These fixed effects capture common attributes of observations that lie in the close proximity (100m) of a common border. They allow us to effectively compare pairs of observations that are close to the same border but receive different grades. We present two sets of standard errors. Our preferred specification clusters at the border and county levels to account for spatial correlation within counties. The other and less conservative specification clusters only at the border level.

To summarize our results in a more parsimonious way, we regress the following equation, which simply reports a single coefficient β that captures the effects of lying in a lower-graded side:

$$\text{Climate Risk}_i = \alpha + \beta LGS_i + f_b + \epsilon_i, \quad (2)$$

where LGS_i is an indicator for whether cell or property i is on the lower-graded side of the nearest HOLC border.

3 Results

3.1 Effects of Redlining on Climate Risks

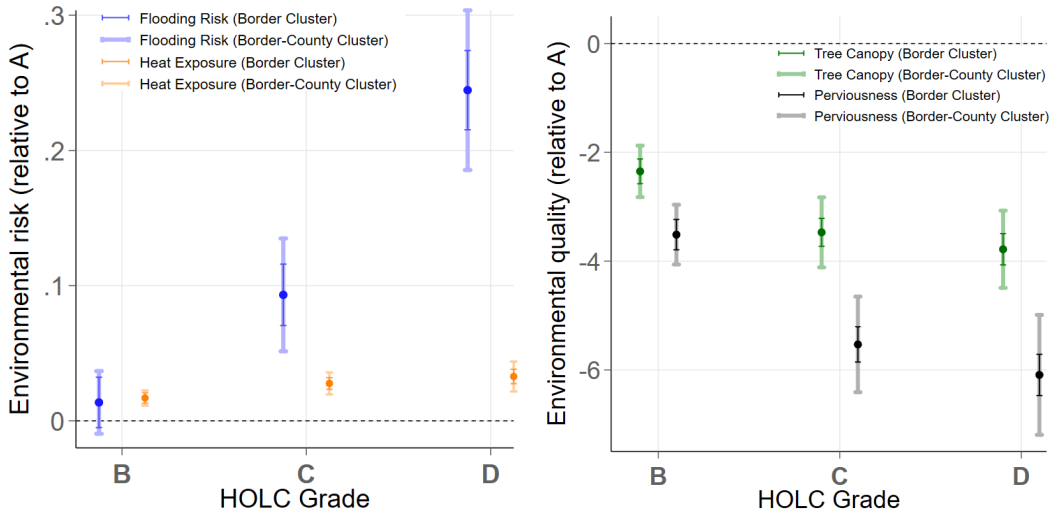
The left panel of Figure 2a plots the point estimates along with 95% confidence intervals for $\hat{\beta}_B, \hat{\beta}_C, \hat{\beta}_D$ from equation (1) (the top panel of Table S11 reports these estimates). The figure shows that the flood risk and heat risk of properties increases monotonically as the HOLC grade worsens. Properties in C-graded areas have a flood factor that is 0.093 points higher than properties in A-graded areas. This effect almost triples for properties in D-graded areas, which have a flood factor that is 0.245 points higher than A-graded properties. These estimates are economically significant, amounting to about 5% and 13% of the sample standard deviation for the flood risk. Similarly, we see that the heat factor increases as HOLC grade worsens, but the magnitudes are smaller than the estimates for the flood factor, which is expected due to the diffusivity of heat. Compared to properties in A-graded polygons, C-graded and D-graded properties have heat factors that are respectively 0.028 and 0.033 points higher.

Similarly, the bottom left panel in Figure 2b plots the coefficients for LGS_i in equation (2) using flooding risk and heat exposure as dependent variables (the bottom panel of Table S11 reports the estimates and standard errors). Being on the lower-graded side of a HOLC border has a statistically and economically significant impact on a property's flood factor, increasing it by 0.1 points, which is about 5% of the sample standard deviation and 5.5% of the sample mean of the flood factor. Similarly, being on the lower-graded side also increases exposure to heat: properties on the lower-graded side have heat factors that are 0.011 points higher than properties on the higher-graded side of the border. As expected, the difference in heat factors is statistically significant but relatively small in magnitude when compared to the difference in flood factors.

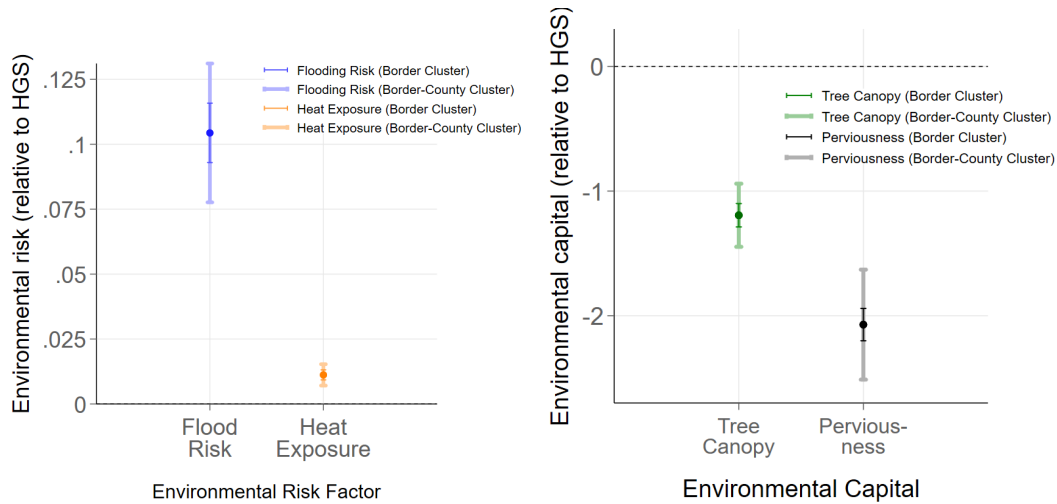
3.2 Role of Environmental Capital

We now explore potential mechanisms contributing to the higher environmental risk in lower-graded HOLC areas. We explore the idea that redlining lowers investment in environmental capital, which then manifests into higher environmental risks.

Intuitively, the community in a neighborhood can invest in local public goods that reduce environmental risk. For example, they could increase the tree coverage and reduce their heat exposure by investing in parks and public gardens. Likewise, they could invest in draining systems or in better and more pervious materials to reduce their risk of flooding. However, a lower HOLC grade can reduce community investments in environmental capital for several reasons. For example, lower property values can affect local taxes and the ability of communities to invest in vegetation, trees, and better construction materials.³²⁻³⁴ Further, areas



(a) EFFECTS OF HOLC GRADES (B, C, D RELATIVE TO A). The left panel plots point estimates $\hat{\beta}_B, \hat{\beta}_C,$ and $\hat{\beta}_D$ from regressing $\text{Climate Risk}_i = \alpha + \beta_B B_i + \beta_C C_i + \beta_D D_i + f_b + \epsilon_i$ using flood risk and heat exposure as dependent variables. The right panel plots point estimates from regressing $\text{Environmental Capital}_i = \alpha + \beta_B B_i + \beta_C C_i + \beta_D D_i + f_b + \epsilon_i$ using tree canopy and perviousness as dependent variables. The figures also plot 95% confidence intervals from two sets of standard errors. The intervals associated with two-way clustering are shown with a solid color and the intervals associated with one-way clustering are shown with transparency. See Table SII for point estimates and standard errors.



(b) EFFECTS OF BEING ON A LOWER-GRADED SIDE (LGS). The left panel plots point estimates for $\hat{\beta}$ from regressing $\text{Climate Risk}_i = \alpha + \beta LGS_i + f_b + \epsilon_i$ using flood risk and heat exposure as dependent variables. The right panel plots estimates from regressing $\text{Environmental Capital}_i = \alpha + \beta LGS_i + f_b + \epsilon_i$ using tree canopy and perviousness as dependent variables. The figures also plot 95% confidence intervals from two sets of standard errors. See Table SII for the point estimates and standard errors.

Figure 2: EFFECTS OF HISTORICAL HOLC GRADES ON CURRENT EXPOSURE TO CLIMATE RISKS AND CURRENT ENVIRONMENTAL CAPITAL.

with high income inequality have been linked to lower levels of social capital and community engagement,³⁵⁻³⁷ which could impede a community’s investment in public goods. Although community investments are difficult to quantify directly, we view our indices of perviousness and tree canopy as informative and observable proxies for the ability of a community to make such investments.

The right panel in Figure 2a reports estimates of equation (1) using our two measures of environmental capital as dependent variables (these results are also reported in the top panel of Table SII). We find that lower HOLC grades lead to reduced perviousness and tree canopy. Cells in B-graded and D-graded areas have a level of perviousness 3.5 and 6.1 percentage points lower, respectively, than cells in A-graded areas on the opposite side of the HOLC border. These effects are large when compared to an average perviousness of 45.7% in our sample. Likewise, cells in D-graded areas have a tree canopy 3.8 percentage points lower than cells in A-graded areas. These effects are also sizable relative to the sample mean of 13.1% in Table 1.

The right panel of Figure 2b reports estimates of equation (2) using our two measures of environmental capital as dependent variables (these results are also reported in the bottom panel of Table SII). We find that a lower HOLC grade reduces perviousness by 2.1 percentage points and tree canopy by 1.2 percentage points. These effects are sizable at 5 to 15% of their sample means.

3.3 Robustness Checks

3.4 Controlling for Location Fundamentals

Table 2 pointed to small or no differences in location fundamentals across opposite sides of the HOLC borders, providing support for the continuity assumption. A complementary exercise to show that our results are not confounding any potential differences in geography across borders is to directly control for location fundamentals in equations (1) and (2). Table SI2 reports our estimates from this exercise. The estimates for the different HOLC grades remain unchanged across all outcomes, showing that location fundamentals do not bias our estimates in any meaningful way.

3.4.1 Using Only Idiosyncratic Borders

A potential concern regarding our identification strategy is that some of the HOLC borders were not randomly drawn. In particular, in several instances, the Home Owners’ Loan Corporation might have drawn these borders considering preexisting socioeconomic and demographic characteristics in the 1930s.^{2,3} These differences can invalidate the continuity assumption if they persist and impact contemporary environmental risk.

To address this concern, we repeat our analysis for a subset of borders that do not exhibit differences in housing and demographic characteristics across opposite sides. The assumption is that the pre-trend concern is alleviated in this subsample of borders, which are arguably closer to being drawn randomly in response to idiosyncratic factors that are not related to housing or demographic characteristics of the neighborhoods. Leveraging an existing methodology from the literature,³ we run a probit regression to predict the likelihood that there is a change in grade at a particular border as a function of differences in socioeconomic and demographic characteristics across sides (see Section [SI.2.2](#) for more details). Demographic and socioeconomic variables include the share of African American population, homeownership rate, log rent, log house value, and the share of foreign-born population obtained from historical census data from 1910, 1920, and 1930.³ We identify idiosyncratic borders as those with propensity scores below the sample median. Intuitively, borders with low propensity scores are less likely to be informed by differences in socioeconomic and demographic characteristics across its sides and are therefore more likely to be drawn in response to idiosyncratic reasons. Out of the 3,403 borders for which we have historical data for, this procedure identifies 1,536 as idiosyncratic.

Table [SI3](#) provides summary statistics for our environmental risk variables for this subsample of borders. Reassuringly, the average exposure to environmental risk for these idiosyncratic borders is similar to the full sample.

Table [SI4](#) reports the results from estimating (1) and (2) for the idiosyncratic border sample. As before, we keep only observations that fall within 100m of these borders. The results using the idiosyncratic border sample are comparable to those reported for the full sample. For example, we estimate that receiving a lower HOLC grade increases flood risk by 0.085 and heat exposure by 0.011 (comparable to the 0.104 and 0.011 reported in Table [SI1](#)). We also find that receiving a lower HOLC grade reduces tree canopy by 0.63 percentage points and perviousness by 0.87 percentage points (similar, though somewhat smaller than the 1.2 percentage points and 2.1 reported in Table [SI1](#)). While comparable in magnitudes, the estimates from the idiosyncratic border sample are slightly less precise due to the fact that we have fewer observations. Altogether, the findings from this exercise support the view that redlining had a detrimental impact on environmental risk and capital and suggests that this effect is not merely a reflection of preexisting socioeconomic differences.

3.4.2 Alternate Buffer Zones

We also explore the robustness of our results using different buffer sizes. Our main results focus on observations lying within 100m of the HOLC borders. Table [SI5](#), [SI6](#), [SI7](#) report estimates for a 50m, 200m, and 300m buffer, respectively. Overall, the results remain comparable when

³We thank Dan Aaronson, Dan Hartley, and Leah Plachinski for sharing these data.

we vary the size of the buffer. In particular, in these two samples, we continue to estimate a significant negative effect of a lower HOLC grade on environmental risk and capital.

3.4.3 Controlling for Housing Prices

In a final check, we explore the robustness of our estimates to controlling for differences in housing prices across HOLC borders. This exercise addresses the concern that redlined areas might have a housing stock of lower quality, which could then lead to lower investments in environmental capital and higher risk. We use the average housing price index for each census tract from 2016-2019 obtained from the Federal Housing Finance Agency. Table S18 reports estimates for equations (1) and (2) controlling for differences in housing prices. We find that controlling for housing prices does not affect our estimates of having a lower HOLC grade.⁴ These results confirm a detrimental of redlining even when opposite sides of a HOLC border share a comparable housing stock.

4 Conclusion

This study offers compelling evidence of the lasting impact of historical redlining policies on contemporary exposure to climate risks, specifically flooding and extreme heat. By leveraging a quasi-experimental design facilitated by the differential assignment of HOLC grades along contiguous boundaries, our analysis reveals a 5.5% increase in flood risk and a smaller but statistically significant increase in heat risk for properties situated on the lower-graded side of a HOLC boundary.

The societal implications of our findings are twofold. First, the unequal distribution of environmental risks exacerbates existing economic disparities. Communities facing elevated risks of flooding and extreme heat are more susceptible to financial strains arising from health-care spending shocks, property damage, and other environmental disasters. Second, the study illuminates the root causes of unequal climate risk exposure, underlining the necessity of an interdisciplinary approach to public policy that merges historical context, social justice, and climate science. This is particularly relevant as initiatives to modernize the Community Reinvestment Act and other federal policies gain momentum.⁹ Our study underscores the importance of incorporating climate resilience measures in these reforms to redress long-standing environmental injustices.

We identify reduced investments in environmental capital, such as tree canopy and ground surface perviousness, as a significant mechanism contributing to the increased environmental risks in lower-graded areas. This enriches our understanding of how past discriminatory

⁴Because lower housing prices are a result of redlining, these results should be interpreted with a degree of caution, as the inclusion of the housing price control could introduce selection bias.³⁸

policies continue to shape present-day vulnerabilities and offers actionable insights for policy-makers aiming to mitigate the multi-dimensional impacts of climate change.

For future work, several promising avenues of inquiry arise from our findings. First, other work can expand the concept of environmental capital to include more nuanced, localized measures such as street-level vegetation, air quality, and access to green spaces. This would enable a more detailed understanding of how environmental quality mediates exposure to climate risks, thereby providing more targeted policy recommendations. Second, a longitudinal analysis could offer insights into how the enduring impacts of redlining are static or exacerbating over time. Such temporal analysis would also gauge the effectiveness of policy interventions aimed at risk mitigation. These extensions would add important dimensions to our understanding of the lingering effects of redlining, further informing policy interventions.

References

- [1] Kenneth T Jackson. Race, ethnicity, and real estate appraisal: The home owners loan corporation and the federal housing administration. *Journal of Urban History*, 6(4):419–452, 1980.
- [2] Daniel Aaronson, Daniel Hartley, and Bhashkar Mazumder. The effects of the 1930s HOLC “redlining” maps. *American Economic Journal: Economic Policy*, 13(4):355–92, 2021.
- [3] Daniel Aaronson, Jacob Faber, Daniel Hartley, Bhashkar Mazumder, and Patrick Sharkey. The long-run effects of the 1930s HOLC “redlining” maps on place-based measures of economic opportunity and socioeconomic success. *Regional Science and Urban Economics*, 86:103622, 2021.
- [4] Lauren J Krivo and Robert L Kaufman. Housing and wealth inequality: Racial-ethnic differences in home equity in the United States. *Demography*, 41(3):585–605, 2004.
- [5] Stephen L Ross and John Yinger. *The color of credit: Mortgage discrimination, research methodology, and fair-lending enforcement*. MIT press, 2002.
- [6] Margery Austin Turner. *Discrimination in Metropolitan Housing Markets: Phase 2 – Asians and Pacific Islanders*. DIANE Publishing, 2003.
- [7] Ian Appel and Jordan Nickerson. Pockets of poverty: The long-term effects of redlining. Available at SSRN 2852856, 2016.
- [8] Scott Markley. Federal ‘redlining’ maps: A critical reappraisal. *Urban Studies*, 2023.

- [9] Federal Deposit Insurance Corporation. Proposed Rule on Community Reinvestment Act, June 2022.
- [10] Spencer Banzhaf, Lala Ma, and Christopher Timmins. Environmental justice: Establishing causal relationships. *Annual Review of Resource Economics*, 11:377–398, 2019.
- [11] Spencer Banzhaf, Lala Ma, and Christopher Timmins. Environmental justice: The economics of race, place, and pollution. *Journal of Economic Perspectives*, 33(1):185–208, 2019.
- [12] Ying-ying Li, Hao Zhang, and Wolfgang Kainz. Monitoring patterns of urban heat islands of the fast-growing Shanghai metropolis, China: Using time-series of Landsat TM/ETM+ data. *International Journal of Applied Earth Observation and Geoinformation*, 19:127–138, 2012.
- [13] Amélie Y. Davis, Jinha Jung, Bryan C. Pijanowski, and Emily S. Minor. Combined vegetation volume and “greenness” affect urban air temperature. *Applied Geography*, 71:106–114, 2016.
- [14] Qingfu Xiao and E Gregory McPherson. Rainfall interception by Santa Monica’s municipal urban forest. *Urban Ecosystems*, 6(4):291–302, 2002.
- [15] Wenfei Xu. Legacies of Institutionalized Redlining: A Comparison Between Speculative and Implemented Mortgage Risk Maps in Chicago, Illinois. *Housing Policy Debate*, 32(2):249–274, mar 2022.
- [16] Price Fishback, Jonathan Rose, Kenneth A Snowden, and Thomas Storrs. New evidence on redlining by federal housing programs in the 1930s. *Journal of Urban Economics*, page 103462, 2022.
- [17] Jacob Krimmel. Persistence of prejudice: Estimating the long term effects of redlining. *Working Paper*, 2018.
- [18] Jacob W. Faber. We built this: Consequences of New Deal era intervention in America’s racial geography. *American Sociological Review*, 85(5):739–775, 2020.
- [19] Jackson Voelkel, Dana Hellman, Ryu Sakuma, and Vivek Shandas. Assessing Vulnerability to Urban Heat: A Study of Disproportionate Heat Exposure and Access to Refuge by Socio-Demographic Status in Portland, Oregon. *International Journal of Environmental Research and Public Health*, 15(4), 2018.
- [20] Angel Hsu, Glenn Sheriff, Tirthankar Chakraborty, and Diego Manya. Disproportionate exposure to urban heat island intensity across major US cities. *Nature Communications*, 12(1):1–11, 2021.

- [21] Roger Renteria, Sara Grineski, Timothy Collins, Aaron Flores, and Shaylynn Trego. Social disparities in neighborhood heat in the Northeast United States. *Environmental Research*, 203:111805, 2022.
- [22] Abdulrahman Jbaily, Xiaodan Zhou, Jie Liu, Ting Hwan Lee, Leila Kamareddine, Stéphane Verguet, and Francesca Dominici. Air pollution exposure disparities across US population and income groups. *Nature*, 601(7892):228–233, 2022.
- [23] Jonathan Colmer, Ian Hardman, Jay Shimshack, and John Voorheis. Disparities in PM2.5 air pollution in the United States. *Science*, 369(6503):575–578, 2020.
- [24] Laura A Bakkensen and Lala Ma. Sorting over flood risk and implications for policy reform. *Journal of Environmental Economics and Management*, 104:102362, 2020.
- [25] Bev Wilson. Urban heat management and the legacy of redlining. *Journal of the American Planning Association*, 86(4):443–457, 2020.
- [26] Jeremy S Hoffman, Vivek Shandas, and Nicholas Pendleton. The effects of historical housing policies on resident exposure to intra-urban heat: A study of 108 US urban areas. *Climate*, 8(1):12, 2020.
- [27] First Street Foundation. The 3rd National Flood Risk Assessment: Infrastructure on the Brink, 2021.
- [28] First Street Foundation. First Street Foundation flood model: Technical methodology document, 2020.
- [29] First Street Foundation. First Street Foundation extreme heat model: Technical methodology document, 2022.
- [30] Thomas J Holmes. The effect of state policies on the location of manufacturing: Evidence from state borders. *Journal of Political Economy*, 106(4):667–705, 1998.
- [31] Sandra E Black. Do better schools matter? Parental valuation of elementary education. *The Quarterly Journal of Economics*, 114(2):577–599, 1999.
- [32] Kirsten Schwarz, Michail Fragkias, Christopher G. Boone, Weiqi Zhou, Melissa McHale, J. Morgan Grove, Jarlath O’Neil-Dunne, Joseph P. McFadden, Geoffrey L. Buckley, Dan Childers, Laura Ogden, Stephanie Pincetl, Diane Pataki, Ali Whitmer, and Mary L. Cadenasso. Trees grow on money: Urban tree canopy cover and environmental justice. *PloS One*, 10(4):e0122051, 2015.

- [33] Diane Hope, Corinna Gries, David Casagrande, Charles L Redman, Nancy B Grimm, and Chris Martin. Drivers of spatial variation in plant diversity across the Central Arizona-Phoenix ecosystem. *Society and Natural Resources*, 19(2):101–116, 2006.
- [34] Ann P Kinzig, Paige Warren, Chris Martin, Diane Hope, and Madhusudan Katti. The effects of human socioeconomic status and cultural characteristics on urban patterns of biodiversity. *Ecology and Society*, 10(1), 2005.
- [35] Alberto Alesina and Eliana La Ferrara. Participation in heterogeneous communities. *The Quarterly Journal of Economics*, 115(3):847–904, 2000.
- [36] Alberto Alesina and Eliana La Ferrara. Who trusts others? *Journal of Public Economics*, 85(2):207–234, 2002.
- [37] Laurie E Paarlberg, Michele Hoyman, and Jamie McCall. Heterogeneity, income inequality, and social capital: A new perspective. *Social Science Quarterly*, 99(2):699–710, 2018.
- [38] Joshua D Angrist and Jörn-Steffen Pischke. *The Wages of Schooling*, chapter 6, pages 209–244. Princeton University Press, 2014.

SI.1 Supplementary Information: Data

Data Availability

We have provided web links to all publicly available data used in our analysis in Section 2.1. The First Street Foundation flood data are confidential and cannot be shared publicly. The historical census data obtained from Aaronson et al. (2021) can also not be shared publicly.

Code Availability

Upon publication, the codes used in the analysis the paper will be shared.

SI.1.1 Full List of Cities

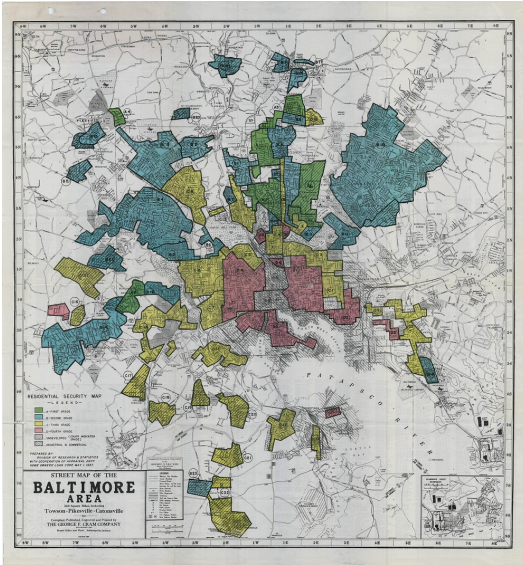
The complete list of cities in our sample is below.

- Alabama: Birmingham, Mobile, Montgomery.
- Arkansas: Little Rock.
- Arizona: Phoenix.
- California: Fresno, Los Angeles, Oakland, Sacramento, San Diego, San Francisco, San Jose, Stockton.
- Colorado: Denver, Pueblo.
- Connecticut: Hartford, New Britain, New Haven, Stamford, Darien, New Canaan, Waterbury.
- Florida: Jacksonville, Miami, St. Petersburg, Tampa.
- Georgia: Atlanta, Augusta, Columbus, Macon, Savannah.
- Iowa: Council Bluffs, Davenport, Des Moines, Dubuque, Sioux City, Waterloo.
- Illinois: Aurora, Chicago, Decatur, East St. Louis, Joliet, Peoria, Rockford, Springfield.
- Indiana: Evansville, Fort Wayne, Indianapolis, Lake Co. Gary, Muncie, South Bend, Terre Haute.
- Kansas: Topeka, Wichita.
- Kentucky: Covington, Lexington, Louisville.
- Louisiana: New Orleans, Shreveport.

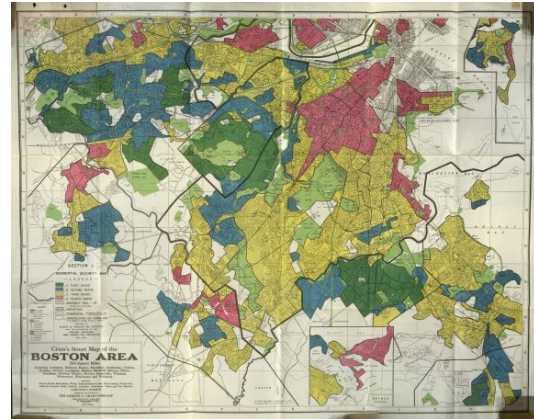
- Massachusetts: Arlington, Belmont, Boston, Braintree, Brockton, Brookline, Cambridge, Chelsea, Dedham, Everett, Haverhill, Holyoke Chicopee, Lexington, Malden, Medford, Melrose, Milton, Needham, Newton, Quincy, Revere, Saugus, Somerville, Waltham, Watertown, Winchester, Winthrop.
- Maryland: Baltimore.
- Michigan: Battle Creek, Bay City, Detroit, Flint, Grand Rapids, Jackson, Kalamazoo, Lansing, Muskegon, Pontiac, Saginaw.
- Minnesota: Duluth, Minneapolis, Rochester, St. Paul.
- Missouri: Greater Kansas City, Springfield, St. Joseph, St. Louis.
- Mississippi: Jackson.
- North Carolina: Asheville, Charlotte, Durham, Greensboro, Winston-Salem.
- Nebraska: Lincoln, Omaha.
- New Hampshire: Manchester.
- New Jersey: Atlantic City, Bergen Co., Camden, Essex Co., Hudson Co., Trenton, Union Co.
- New York: Albany, Binghamton-Johnson City, Bronx, Brooklyn, Buffalo, Elmira, Lower Westchester Co., Manhattan, Niagara Falls, Poughkeepsie, Queens, Rochester, Schenectady, Staten Island, Syracuse, Troy, Utica.
- Ohio: Akron, Canton, Cleveland, Columbus, Dayton, Hamilton, Lima, Lorain, Portsmouth, Springfield, Toledo, Warren, Youngstown.
- Oklahoma: Oklahoma City, Tulsa.
- Oregon: Portland.
- Pennsylvania: Altoona, Bethlehem, Chester, Erie, Harrisburg, Johnstown, Lancaster, New Castle, Philadelphia, Pittsburgh, Wilkes-Barre, York.
- Rhode Island: Pawtucket & Central Falls, Providence, Woonsocket.
- South Carolina: Columbia.
- Tennessee: Chattanooga, Knoxville, Memphis, Nashville.
- Texas: Amarillo, Austin, Beaumont, Dallas, El Paso, Fort Worth, Galveston, Houston, Port Arthur, San Antonio, Waco.

- Utah: Ogden, Salt Lake City.
- Virginia: Lynchburg, Newport News, Norfolk, Richmond, Roanoke.
- Washington: Seattle, Spokane, Tacoma.
- Wisconsin: Kenosha, Madison, Milwaukee Co., Oshkosh, Racine.
- West Virginia: Charleston, Huntington, Wheeling.

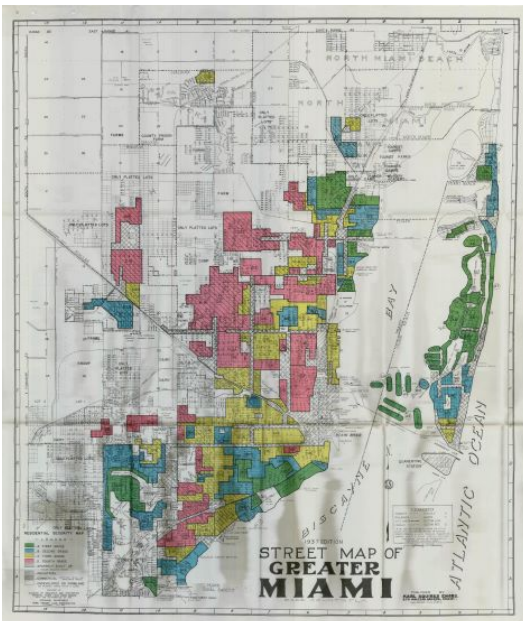
SI.1.2 HOLC Maps: Examples



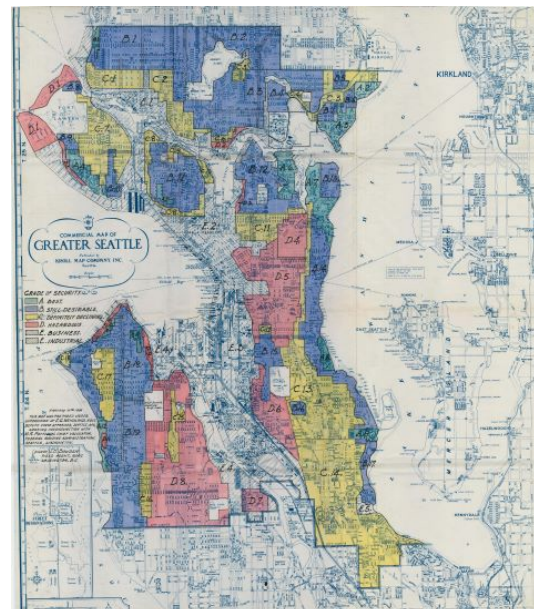
(a) Baltimore



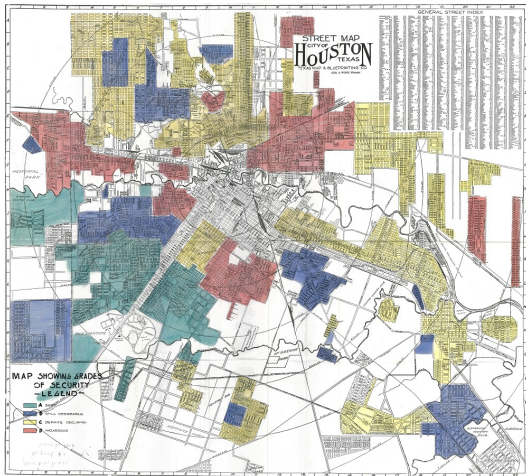
(b) Boston



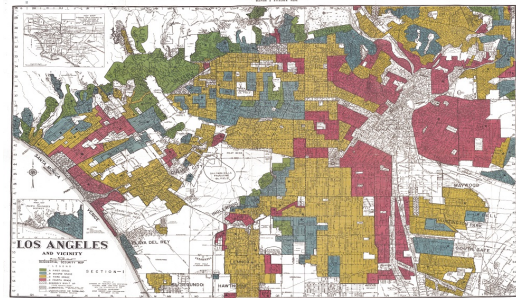
(c) Miami



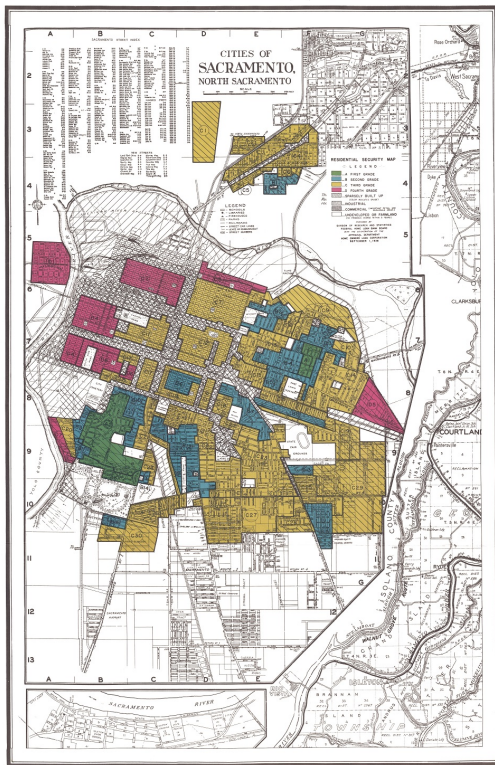
(d) Seattle



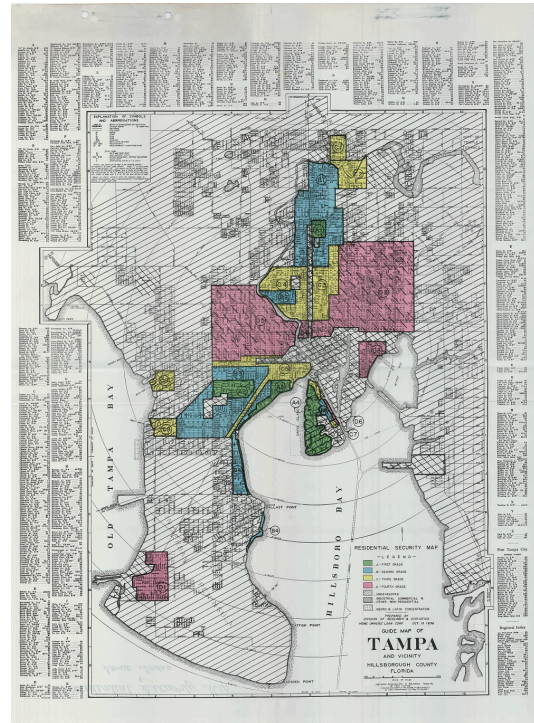
(e) Houston



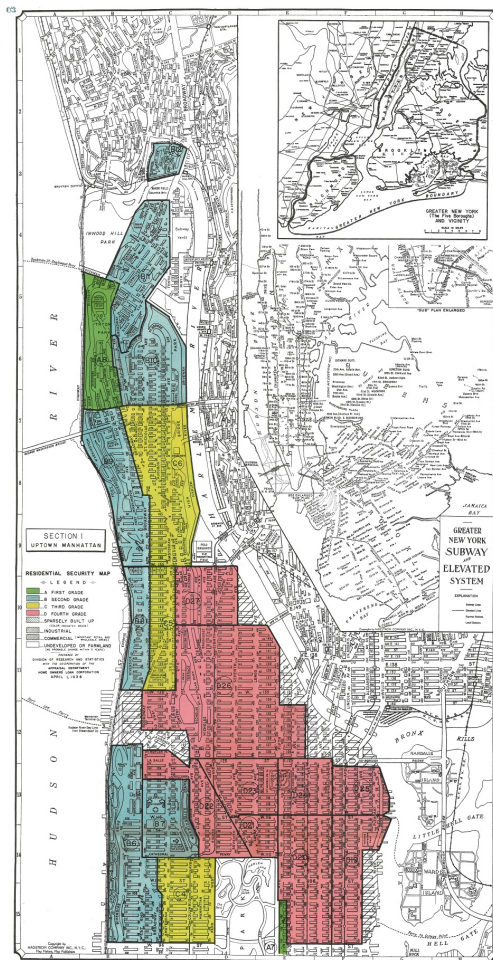
(f) Los Angeles



(g) Sacramento



(h) Tampa

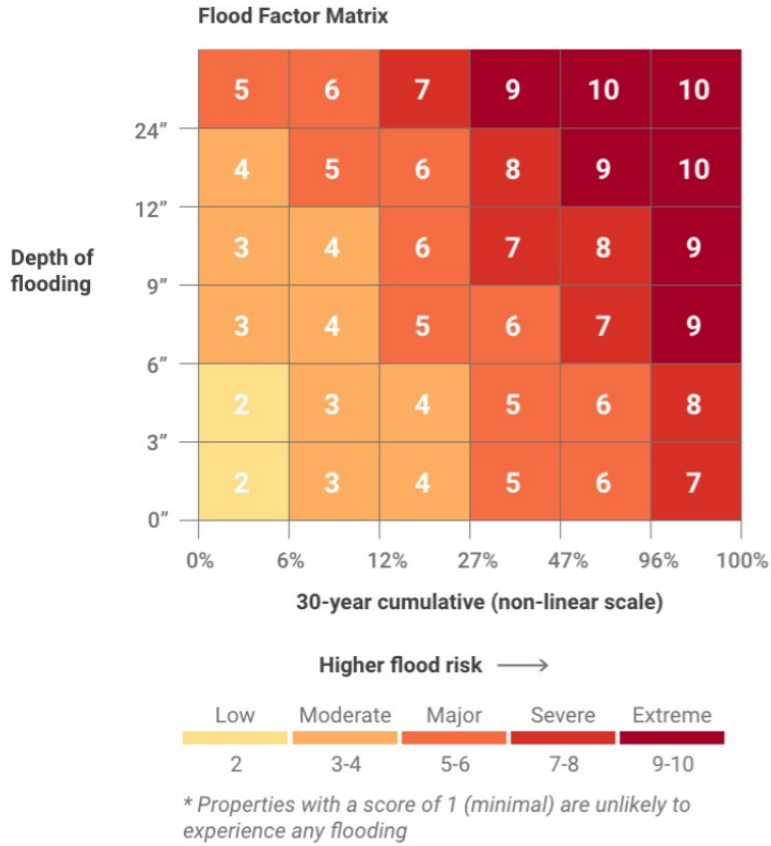


(i) Manhattan

Figure SI1: Examples of HOLC Map Scans

SI.1.3 Environmental Risk Factors

(a) FLOOD FACTOR MATRIX.



(b) HEAT FACTOR MATRIX.

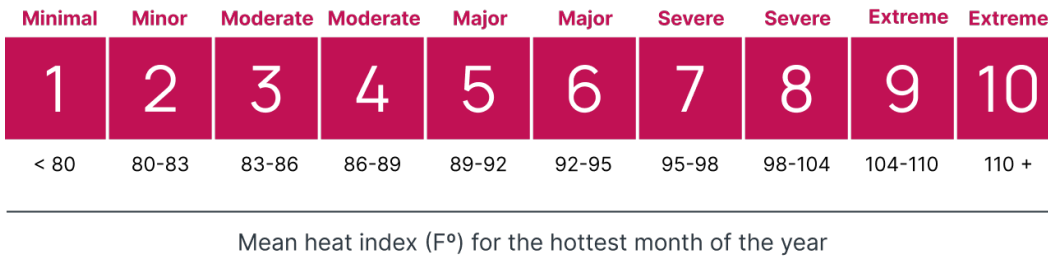


Figure SI2: The top matrix provides an illustration of how the flood factor risk score is assigned to each property. The measure increases as depth of flooding increases or as likelihood of flooding increases. The flood factor is calculated from the First Street Foundation Flood Model. The bottom matrix provides an illustration of how to interpret the heat factor for each property. The heat factor is calculated from the First Street Foundation Extreme Heat Model.

SI.2 Supplementary Information: Omitted Tables

Table SI1: Effects of Historical HOLC Grade on Current Environmental Risk and Capital

	(I) Flood Factor	(II) Heat Factor	(III) % Canopy	(IV) % Pervious
<i>Panel A. Estimates of equation (1)</i>				
B Grade	0.014 (0.010) [0.012]	0.017 (0.002)*** [0.003]***	-2.350 (0.116)*** [0.242]***	-3.513 (0.143)*** [0.280]***
C Grade	0.093 (0.012)*** [0.021]***	0.028 (0.002)*** [0.004]***	-3.471 (0.131)*** [0.329]***	-5.531 (0.165)*** [0.449]***
D Grade	0.245 (0.015)*** [0.030]***	0.033 (0.003)*** [0.006]***	-3.782 (0.147)*** [0.362]***	-6.091 (0.193)*** [0.563]***
N	2,005,273	2,007,785	2,353,043	2,353,043
R^2	0.629	0.991	0.562	0.593
<i>Panel B. Estimates of equation (2)</i>				
LGS (Lower-Graded Side)	0.104 (0.006)*** [0.014]***	0.011 (0.001)*** [0.002]***	-1.194 (0.048)*** [0.129]***	-2.071 (0.066)*** [0.225]***
N	2,005,273	2,007,785	2,353,043	2,353,043
R^2	0.629	0.991	0.561	0.592

Note.— The top panel shows that flood risk, heat risk, canopy coverage, and perviousness all worsen as HOLC grade worsens. The top panel shows the results from equation (1) using properties and cells within 100m of nearest HOLC border. The bottom panel shows properties/cells on a lower HOLC graded side have worse flood risk, heat risk, perviousness, and canopy coverage than those on a higher-graded side. The bottom panel shows the results from equation (2) within 100m of nearest HOLC border. Standard errors clustered at the border level in parentheses. Standard errors clustered at the border and county levels are in square brackets. *** $p < 0.01$, ** $p < 0.05$, * $p < 0.1$.

Table SI2: Effects of Historical HOLC Grade on Current Environmental Risk and Capital Controlling for Location Fundamentals

	(I) Flood Factor	(II) Heat Factor	(III) % Canopy	(IV) % Pervious
<i>Panel A. Estimates of equation (1)</i>				
B Grade	0.013 (0.010) [0.012]	0.017 (0.002)*** [0.003]***	-2.342 (0.116)*** [0.241]***	-3.501 (0.142)*** [0.279]***
C Grade	0.091 (0.012)*** [0.021]***	0.027 (0.002)*** [0.004]***	-3.458 (0.131)*** [0.328]***	-5.510 (0.165)*** [0.446]***
D Grade	0.241 (0.015)*** [0.030]***	0.032 (0.003)*** [0.006]***	-3.766 (0.147)*** [0.361]***	-6.062 (0.193)*** [0.558]***
<i>Controls:</i>				
Elevation	✓	✓	✓	✓
Precipitation	✓	✓	✓	✓
Slope	✓	✓	✓	✓
N	2,005,236	2,007,748	2,353,043	2,353,043
R2	0.629	0.991	0.562	0.593
<i>Panel B. Estimates of equation (2)</i>				
LGS	0.103 (0.006)*** [0.013]***	0.011 (0.001)*** [0.002]***	-1.188 (0.048)*** [0.129]***	-2.06 (0.066)*** [0.223]***
<i>Controls:</i>				
Elevation	✓	✓	✓	✓
Precipitation	✓	✓	✓	✓
Slope	✓	✓	✓	✓
N	2,005,236	2,007,748	2,353,043	2,353,043
R2	0.629	0.991	0.561	0.592

Note.— The top panel shows that flood risk, heat risk, canopy coverage, and perviousness all worsen as HOLC grade worsens. The top panel shows the results from equation (1) using properties and cells within 100m of nearest HOLC border. The bottom panel shows properties/cells on a lower HOLC graded side have worse flood risk, heat risk, perviousness, and canopy coverage than those on a higher-graded side. The bottom panel shows the results from equation (2) within 100m of nearest HOLC border. All columns control for elevation, precipitation, and slope. Standard errors clustered at the border level in parentheses. Standard errors clustered at the border and county levels are in square brackets. *** $p < 0.01$, ** $p < 0.05$, * $p < 0.1$.

SI.2.1 Robustness Checks

SI.2.2 Further Details on Idiosyncratic Borders Exercise

To address the concern that there are pre-trends in certain demographic and housing variables across HOLC borders, we follow the methodology outlined in Aaronson et al. (2021)³ to

identify borders that are plausibly randomly drawn. We construct comparison boundaries that are between polygons that were given the same grade by the HOLC. For the comparison borders, one side is randomly assigned as the lower-graded side and the other the higher-graded side. We pool these boundaries with actual treated borders separating polygons with different grades and estimate the following probit:

$$1\{Treated\}_{b,c} = \alpha_c + \sum_{k=1}^K \beta_{1910}^k z_{b,c}^{k,1910} + \beta_{1920}^k z_{b,c}^{k,1920} + \beta_{1930}^k z_{b,c}^{k,1930} + \epsilon_{b,c}, \quad (3)$$

where $1\{Treated\}_{b,c}$ indicates if border b in city c is a border with a HOLC grade change and $z_{b,c}^{k,t} = x_{lgs,b,c}^{k,t} - x_{hgs,b,c}^{k,t}$ describes the gap in a housing or demographic variable k on the lower-graded side and the higher-graded side at time $t = 1910, 1920, \text{ and } 1930$. As mentioned, the housing and demographic variables indexed by k come from historical decennial censuses and include the share of the population that is African American, the homeownership rate, log rent, log house value, and share foreign born. These data come from the 1910, 1920, and 1930 decennial censuses, which are available from the Minnesota Population Center and Ancestry.com.

Figure SI4 visualizes the fact that the below median propensity score borders exhibit fewer differences in the variables indexed by k before the HOLC borders were drawn. The solid line plots the difference in the share of the population that is African American on the lower-graded side vs higher-graded side for the full sample of borders. There is an increasing positive difference over time on the LGS compared to the HGS. The dashed line plots the difference in the share of African American on the LGS vs the HGS for the below median propensity score sample. The difference reduces to close to zero when we use this sample. Because this sample of borders exhibits fewer pre-trends in certain demographic variables, we run our main analyses on this sample as a robustness check.

Figure SI3: Share of African American on LGS vs HGS in Idiosyncratic Sample.

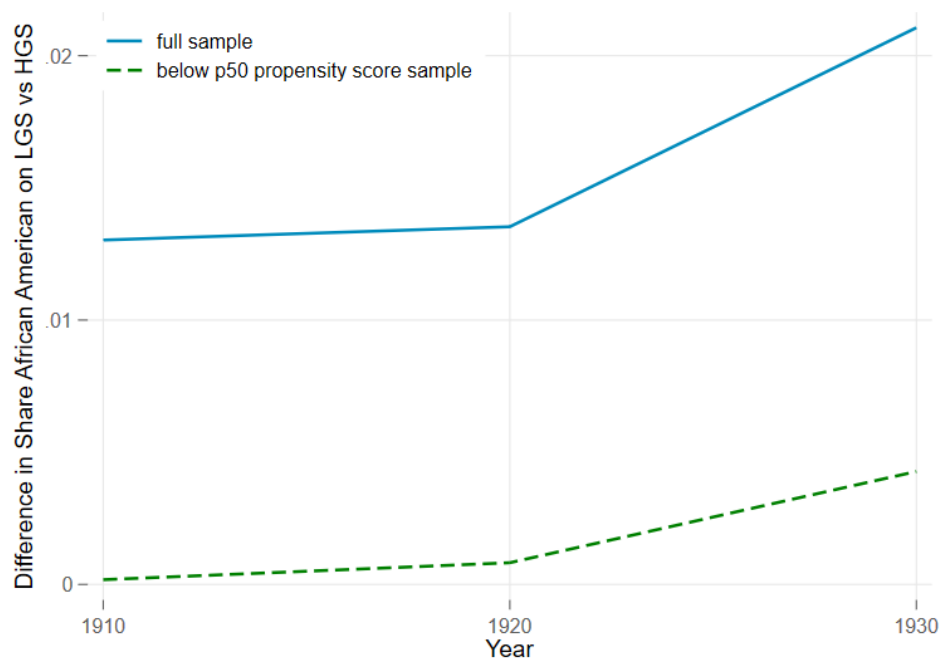


Figure SI4: This figure plots the share of the population that is African American on the LGS vs the HGS of a HOLC border from 1910-1930. The solid line shows the share of African American for the full sample of HOLC borders. The dashed line shows the share of African American for the below median propensity score sample.

Table SI3: Summary statistics for the Idiosyncratic Border Sample

	(I) Full Idiosyncratic Sample	(II) A grade	(III) B grade	(IV) C grade	(V) D grade	(VI) 100m Boundary Sample
<i>Panel A. Environmental Risks</i>						
Flood Factor (1-10)	1.78 (1.92)	1.18 (0.86)	1.60 (1.75)	1.78 (1.91)	1.93 (2.05)	1.83 (2.02)
Observations (properties)	308,521	8,347	52,124	146,390	101,659	118,413
Heat Factor (1-10)	4.92 (1.94)	5.06 (1.53)	4.81 (1.71)	4.85 (1.93)	5.07 (2.09)	4.85 (1.95)
Observations (properties)	308,800	8,350	52,126	146,570	101,753	118,491
<i>Panel B. Environmental Capital</i>						
Tree Canopy (%)	7.21 (13.91)	22.94 (21.58)	8.98 (14.63)	6.86 (13.38)	5.22 (12.05)	7.04 (13.83)
Observations (30m cells)	231,554	7,762	39,976	106,175	77,641	92,534
Perviousness (%)	36.01 (22.10)	54.50 (25.92)	39.55 (22.10)	35.52 (21.46)	33.00 (21.40)	35.02 (22.16)
Observations (30m cells)	231,554	7,762	39,976	106,175	77,641	92,534

Note.— The table provides the mean and standard deviation (in parentheses) for the measures of environmental risk and the proxies for environmental capital using the idiosyncratic border sample. The columns break down these statistics by sample, including all HOLC areas in the idiosyncratic sample, A-graded areas, B-graded areas, C-graded areas, and D-graded areas, respectively. The final column reports these statistics for the 100m boundary sample described in Section 2.

Table SI4: Using Only Idiosyncratic Borders

	(I) Flood Factor	(II) Heat Factor	(III) % Canopy	(IV) % Pervious
<i>Panel A. Estimates of equation (1)</i>				
B Grade	0.066 (0.075) [0.107]	0.031 (0.034) [0.046]	-1.229 (0.761) [1.118]	-0.606 (0.993) [1.579]
C Grade	0.116 (0.089) [0.079]	0.028 (0.035) [0.045]	-1.913 (0.818)** [1.297]	-1.592 (1.076) [1.588]
D Grade	0.212 (0.094)** [0.100]**	0.041 (0.035) [0.041]	-2.402 (0.835)** [1.344]*	-2.299 (1.128)** [1.712]
Idiosyncratic border subsample	✓	✓	✓	✓
N	118,411	118,489	92,534	92,534
R2	0.586	0.986	0.421	0.515
<i>Panel B. Estimates of equation (2)</i>				
LGS	0.085 (0.029)** [0.026]**	0.011 (0.005)** [0.004]**	-0.634 (0.169)** [0.268]**	-0.867 (0.287)** [0.414]**
Idiosyncratic border subsample	✓	✓	✓	✓
N	118,411	118,489	92,534	92,534
R2	0.586	0.986	0.421	0.515

Note.— Table presents the results from equation (1) (top panel) and (2) (bottom panel) using the below median propensity score sample outlined in Section 3.4.1 and SI.2.2. While the estimates become less precise, likely because of the sample size decrease, we still observe that properties and cells on the lower-graded side of a HOLC border with a grade change have higher flood risk and heat exposure and have lower levels of environmental capital compared to properties/cells on the higher-graded side. Standard errors clustered at the border level in parentheses. Standard errors clustered at the border and county levels are in square brackets. *** $p < 0.01$, ** $p < 0.05$, * $p < 0.1$.

Table SI5: 50m Boundary Offset

	(I) Flood Factor	(II) Heat Factor	(III) % Canopy	(IV) % Pervious
<i>Panel A. Estimates of equation (1)</i>				
B Grade	0.012 (0.009) [0.012]	0.008 (0.002)*** [0.002]***	-1.536 (0.108)*** [0.179]***	-2.269 (0.124)*** [0.207]***
C Grade	0.066 (0.011)*** [0.014]***	0.014 (0.002)*** [0.002]***	-2.178 (0.121)*** [0.232]***	-3.499 (0.142)*** [0.300]***
D Grade	0.154 (0.013)*** [0.018]***	0.018 (0.002)*** [0.004]***	-2.309 (0.135)*** [0.246]***	-3.868 (0.168)*** [0.372]***
N	1,041,482	1,042,786	1,277,468	1,277,468
R2	0.689	0.992	0.623	0.656
<i>Panel B. Estimates of equation (2)</i>				
LGS	0.065 (0.005)*** [0.008]***	0.006 (0.001)*** [0.001]***	-0.699 (0.044)*** [0.087]***	-1.296 (0.059)*** [0.146]***
N	1,041,482	1,042,786	1,277,468	1,277,468
R2	0.689	0.992	0.623	0.656

Note.— Table presents results from equations (1) and (2) using a sample that offsets our 100 meter buffer zones by 50 meters on either side of the HOLC border. The top panel shows results from equation (2); the bottom panel shows results from equation (1). Standard errors clustered at the border level in parentheses. Standard errors clustered at the border and county levels are in square brackets. *** $p < 0.01$, ** $p < 0.05$, * $p < 0.1$.

Table SI6: 200m Boundary Sample

	(I) Flood Factor	(II) Heat Factor	(III) % Canopy	(IV) % Pervious
<i>Panel A. Estimates of equation (1)</i>				
B Grade	0.016 (0.011) [0.013]	0.028 (0.002)*** [0.005]***	-3.191 (0.132)*** [0.242]***	-4.615 (0.164)*** [0.280]***
C Grade	0.114 (0.013)*** [0.026]***	0.044 (0.003)*** [0.007]***	-4.708 (0.150)*** [0.329]***	-7.102 (0.192)*** [0.449]***
D Grade	0.300 (0.017)*** [0.040]***	0.051 (0.003)*** [0.009]***	-5.198 (0.167)*** [0.362]***	-7.936 (0.224)*** [0.563]***
N	3,345,957	3,350,165	3,821,716	3,821,716
R2	0.572	0.990	0.518	0.546
<i>Panel B. Estimates of equation (2)</i>				
LGS	0.127 (0.007)*** [0.018]***	0.017 (0.001)*** [0.003]***	-1.643 (0.054)*** [0.129]***	-2.67 (0.076)*** [0.225]***
N	3345957	3350165	3821716	3821716
R2	0.571	0.99	0.517	0.545

Note.— Table presents results from Equations (1) and (2) using properties/cells within 300 meters of the nearest HOLC border with a grade change. The top panel shows results from equation (2); the bottom panel shows results from equation (1). Standard errors clustered at the border level in parentheses. Standard errors clustered at the border and county levels are in square brackets. *** $p < 0.01$, ** $p < 0.05$, * $p < 0.1$.

Table SI7: 300m Boundary Sample

	(I) Flood Factor	(II) Heat Factor	(III) % Canopy	(IV) % Pervious
<i>Panel A. Estimates of equation (1)</i>				
B Grade	0.016 (0.011) [0.013]	0.028 (0.002)*** [0.005]***	-3.191 (0.132)*** [0.242]***	-4.615 (0.164)*** [0.280]***
C Grade	0.114 (0.013)*** [0.026]***	0.044 (0.003)*** [0.007]***	-4.708 (0.150)*** [0.329]***	-7.102 (0.192)*** [0.449]***
D Grade	0.300 (0.017)*** [0.040]***	0.051 (0.003)*** [0.009]***	-5.198 (0.167)*** [0.362]***	-7.936 (0.224)*** [0.563]***
N	3,345,957	3,350,165	3,821,716	3,821,716
R2	0.572	0.990	0.518	0.546
<i>Panel B. Estimates of equation (2)</i>				
LGS	0.127 (0.007)*** [0.018]***	0.017 (0.001)*** [0.003]***	-1.643 (0.054)*** [0.129]***	-2.67 (0.076)*** [0.225]***
N	3345957	3350165	3821716	3821716
R2	0.571	0.99	0.517	0.545

Note.— Table presents results from equations (1) and (2) using properties/cells within 300 meters of the nearest HOLC border with a grade change. The top panel shows results from equation (2); the bottom panel shows results from equation (1). Standard errors clustered at the border level in parentheses. Standard errors clustered at the border and county levels are in square brackets. *** $p < 0.01$, ** $p < 0.05$, * $p < 0.1$.

Table SI8: Controlling for Housing Price Index

	(I) Flood Factor	(II) Heat Factor	(III) % Canopy	(IV) % Pervious
<i>Panel A. Estimates of equation (1)</i>				
B Grade	0.007 (0.011) [0.012]	0.019 (0.002)*** [0.003]***	-2.332 (0.131)*** [0.248]***	-3.519 (0.155)*** [0.300]***
C Grade	0.088 (0.013)*** [0.020]***	0.029 (0.002)*** [0.004]***	-3.468 (0.154)*** [0.344]***	-5.496 (0.184)*** [0.464]***
D Grade	0.259 (0.020)*** [0.037]***	0.030 (0.003)*** [0.005]***	-3.896 (0.183)*** [0.414]***	-6.263 (0.239)*** [0.658]***
Average HPI	-0.000 (0.000)** [0.000]	-0.000 (0.000)*** [0.000]*	0.003 (0.001)*** [0.001]***	0.006 (0.001)*** [0.001]***
N	1,227,626	1,228,974	1,486,961	1,486,961
R2	0.616	0.991	0.584	0.590
<i>Panel B. Estimates of equation (2)</i>				
LGS	0.096 (0.007)*** [0.015]***	0.012 (0.001)*** [0.002]***	-1.387 (0.062)*** [0.159]***	-2.383 (0.083)*** [0.245]***
Average HPI	-0.000 (0.000)** [0.000]*	-0.000 (0.000)*** [0.000]*	0.003 (0.001)*** [0.001]***	0.006 (0.001)*** [0.001]***
N	1227626	1228974	1486961	1486961
R2	0.616	0.991	0.583	0.59

Note.— Table presents results from Equations (1) and (2) for properties and cells in the 100 meter boundary sample with the inclusion of a control for the housing price index (HPI) at the census tract level. The top panel shows results from equation (2); the bottom panel shows results from equation (1). Standard errors clustered at the border level in parentheses. Standard errors clustered at the border and county levels are in square brackets. *** $p < 0.01$, ** $p < 0.05$, * $p < 0.1$.